

Temperature-Dependent Contact of Weakly Interacting Single-Component Fermi Gases and Loss Rate of Degenerate Polar Molecules


Xin-Yuan Gao¹, D. Blume^{2,3}, and Yangqian Yan^{1,4,*}

¹*Department of Physics, The Chinese University of Hong Kong, Shatin, New Territories, Hong Kong, China*

²*Homer L. Dodge Department of Physics and Astronomy, The University of Oklahoma,
440 W. Brooks Street, Norman, Oklahoma 73019, USA*

³*Center for Quantum Research and Technology, The University of Oklahoma, 440 W. Brooks Street, Norman, Oklahoma 73019, USA*

⁴*The Chinese University of Hong Kong Shenzhen Research Institute, 518057 Shenzhen, China*

 (Received 13 March 2023; revised 21 May 2023; accepted 27 June 2023; published 25 July 2023)

Motivated by the experimental realization of single-component degenerate Fermi gases of polar ground state KRb molecules with intrinsic two-body losses [L. De Marco *et al.*, A degenerate Fermi gas of polar molecules, *Science* **363**, 853 (2019).], this work studies the finite-temperature loss rate of single-component Fermi gases with weak interactions. First, we establish a relationship between the two-body loss rate and the p -wave contact. Second, we evaluate the contact of the homogeneous system in the low-temperature regime using p -wave Fermi liquid theory and in the high-temperature regime using the second-order virial expansion. Third, conjecturing that there are no phase transitions between the two temperature regimes, we smoothly interpolate the results to intermediate temperatures. It is found that the contact is constant at temperatures close to zero and increases first quadratically with increasing temperature and finally—in agreement with the Bethe-Wigner threshold law—linearly at high temperatures. Fourth, applying the local-density approximation, we obtain the loss-rate coefficient for the harmonically trapped system, reproducing the experimental KRb loss measurements within a unified theoretical framework over a wide temperature regime without fitting parameters. Our results for the contact are not only applicable to molecular p -wave gases but also to atomic single-component Fermi gases, such as ^{40}K and ^6Li .

DOI: 10.1103/PhysRevLett.131.043401

Introduction.—Ultracold polar molecules possess, thanks to their highly controllable long-range anisotropic interactions, a dipole moment. This, coupled with their rovibrational degrees of freedom, make them promising candidates for quantum computation [1–4] and quantum simulations [5–9]. For example, stable degenerate molecular gases can be used to simulate strongly interacting lattice spin models, providing a promising platform for the study of anyonic excitations [10]. Even though degenerate atomic Bose and Fermi gases are now being produced routinely, the experimental realization of degenerate molecular gases had been, despite impressive progress by many groups [11–23], up until 2019 [24] hampered detrimentally by losses. The experimentally measured loss-rate coefficients were found to increase linearly with the temperature, in nice agreement with predictions derived from two-body physics, i.e., the Bethe-Wigner threshold law [25–28] and multi-channel quantum defect theory [29,30].

In 2019, experimentalists realized molecular $^{40}\text{K}^{87}\text{Rb}$ gases with temperatures T as low as $T/T_F \approx 0.3$, where T_F denotes the Fermi temperature. In a single-component system, the dominant scattering channel is p wave since s -wave collisions are prohibited by the Pauli exclusion principle. Importantly, chemical reactions were found to be suppressed in the quantum degenerate regime, i.e., the

loss-rate coefficient was found to deviate from the linear temperature dependence observed at higher temperatures [24]. Several groups have attempted to explain this intriguing behavior [31,32]: Ref. [31] used the master equation, considered fermionic statistics, intermediate four-body complexes, and other factors while Ref. [32] connected two-body losses to three distinct p -wave contacts. Yet, a robust theoretical formulation that yields convincing agreement with the experimental data over the entire temperature regime is still lacking. What role do quantum statistics and many-body effects play as the temperature drops? Can the losses be linked to microscopic few-body parameters? And, if so, how can this be accomplished?

This Letter theoretically investigates, starting with a non-Hermitian Hamiltonian with p -wave zero-range interactions, the loss-rate coefficient and arrives at predictions that agree well with published experimental observations. Our key findings are as follows. (i) Explicit expressions for the temperature-dependent p -wave contact of the weakly interacting p -wave gas are obtained in terms of the low-energy two-body scattering parameters. (ii) We show that the dominant contribution to the loss rate is—for the experimentally accessible temperature regime—proportional to the p -wave contact [33–37], defined from the p -wave

scattering volume; specifically, effective-range contributions are negligible in the weakly interacting regime considered. (iii) The low- and high-temperature regimes are described by Fermi liquid theory and virial expansion, respectively. Motivated by the conjectured absence of a phase transition at intermediate temperatures, the low- and high-temperature predictions are interpolated smoothly. (iv) Using the local-density approximation, we calculate the loss-rate coefficient of harmonically trapped systems following the experimental procedure [24]. The resulting loss curve depends on a single atomic physics parameter, namely the imaginary part of the p -wave scattering volume, which is known from experimental high-temperature data [38] and multichannel quantum defect theory calculations [30,31]. Our parameter-free theory predictions are in excellent agreement with the experimental data from 2019.

Effective Hamiltonian and loss relation.—For reactive molecular systems such as KRb, two-body losses are triggered by chemical reactions: Two incoming molecules collide and form a four-body complex K_2Rb_2 . Subsequently, the four-body complex breaks up into K_2 and Rb_2 molecules. Since this process converts internal energy to kinetic energy, the K_2 and Rb_2 molecules become untrapped and fly away. It is important to note that the intermediate four-body complexes are transient, with lifetimes of the order of ps at high temperatures [39,40]. Even in recent lifetime-enhancing experimental setups [41,42], the formation and decay of the four-body complexes are still of the order of μ s, which is significantly faster than the ms timescale of interest to us. Thus, we treat the chemical reaction as a non-Hermitian loss process and model the system by an effective non-Hermitian Hamiltonian \hat{H}_{eff} , which is equivalent to a Lindblad master equation formulation where the jump operator L contains a term proportional to $\Psi(\mathbf{r}')\Psi(\mathbf{r})$, annihilating two molecules when their positions \mathbf{r}' and \mathbf{r} are close to each other [43] [$\Psi(\mathbf{r})$ is the fermionic field operator]. Assuming a homogeneous system, the effective Hamiltonian reads as [44]

$$\hat{H}_{\text{eff}} = \int d^3\mathbf{r} \Psi^\dagger(\mathbf{r}) \left(-\frac{\hbar^2 \nabla_{\mathbf{r}}^2}{2m} \right) \Psi(\mathbf{r}) + \frac{1}{2} \int d^3\mathbf{r} d^3\mathbf{r}' \Psi^\dagger(\mathbf{r}) \Psi^\dagger(\mathbf{r}') U(|\mathbf{r} - \mathbf{r}'|) \Psi(\mathbf{r}') \Psi(\mathbf{r}), \quad (1)$$

where U denotes the effective isotropic two-body interaction. Each fermionic KRb molecule is treated as a “fundamental unit” and U describes collisions between two KRb molecules. The non-Hermiticity of \hat{H}_{eff} comes from the imaginary part of U , which models losses due to K_2 and Rb_2 leaving the trap. Defining the particle number operator $\hat{N} = \int d^3\mathbf{r} \Psi^\dagger(\mathbf{r}) \Psi(\mathbf{r})$, the particle loss dN/dt can be related to the imaginary part of the effective Hamiltonian [44], $(dN/dt) = \frac{4}{\hbar} \Im \langle \hat{H}_{\text{eff}} \rangle$, where the average particle number N is given by $\langle \hat{N} \rangle$, with $\langle \cdot \rangle$ denoting the trace.

Without an external electric field, the interaction U between two molecules is of van der Waals type and short ranged. In the low-energy scattering regime, $U(|\mathbf{r} - \mathbf{r}'|)$ can be parameterized by the complex scattering volume v_p , which appears in the leading order term of the low-energy expansion of the p -wave phase shift $\delta_p(k)$, $\tan(\delta_p(k)) = -v_p k^3$. In what follows, we concentrate on the weak-interaction and weak-reaction regimes, in which both the real and imaginary parts of v_p are significantly smaller than $1/n = V/N$, where n and V denote the density and volume, respectively. In this limit, we find [44] that the loss rate can be expressed in terms of the scattering volume v_p and the p -wave contact C_v conjugate to v_p ,

$$\frac{dN}{dt} = \frac{6\hbar}{m} C_v \frac{\Im(v_p)}{[\Re(v_p)]^2}; \quad (2)$$

here, $C_v = -(2m/3\hbar^2) \partial F[\Re(v_p)] / \partial v_p^{-1}$ [33–37] and F denotes the Helmholtz free energy and m the mass of the Fermi gas constituents. Since the contact C_v , which is an extensive variable, is evaluated using the real part of v_p , and not the complex v_p , C_v is purely real. The physical picture behind the derivation is that the system first thermalizes and that losses are subsequently turned on perturbatively. Equation (2) is analogous to the universal loss relation for s -wave systems, where the loss is proportional to the s -wave contact [43,59,60].

Effective range.—The low-energy properties of strongly interacting p -wave systems do not only depend on v_p but also on the effective range R [33], which appears at subleading order in the low-energy expansion, $\tan[\delta_p(k)] = -v_p k^3 + R^{-1} v_p^2 k^5$. Assuming the naturalness of the expansion in the weakly interacting regime (this means that v_p and R are, respectively, proportional to l_0^3 and l_0 , where l_0 is the characteristic length of the interaction), the effective-range contribution to the thermodynamics can be neglected. This follows because $|R^{-1} v_p^2| k^5$ is a factor of $l_0^2 k^2$ smaller than $|v_p| k^3$. Setting l_0 equal to the van der Waals length of KRb molecules ($l_0 \simeq 118a_0$) [30], the quantity $l_0^2 k^2$, in turn, can be shown to be much smaller than 1 for the experimental temperature of several hundred nK [24]. The above argument can be extended to justify dropping contributions from other higher-order terms in the expansion of the phase shift, which may, e.g., arise from the van der Waals tail of the interaction [61,62].

Our conclusion is consistent with the literature. First, at zero temperature, the leading-order contribution to the energy—calculated within the Fermi liquid theory—does not depend on the effective range [63]. Second, at high temperatures, the loss-rate coefficient scales linearly with $\Im(v_p)T$. Third, the fact that a T^2 scaling, which arises from effective-range contributions based on dimensional arguments, is not observed experimentally [38] additionally supports that effective-range contributions play a minor role.

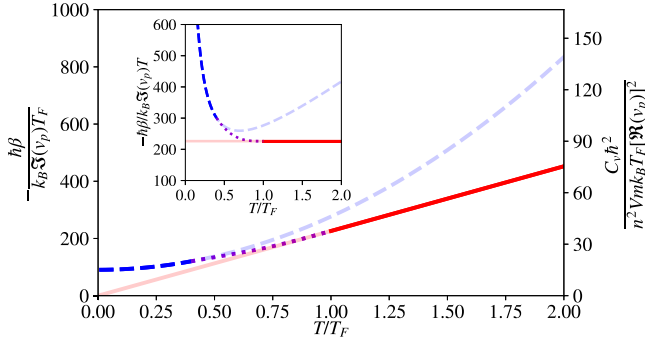


FIG. 1. The loss-rate coefficient β (left axis) and contact C_v (right axis) as a function of the temperature T . Blue dashed and red solid lines are obtained from the Fermi liquid theory and the second-order virial expansion, respectively. Transparent lines extend the predictions beyond their range of validity. The purple dotted line interpolates the low- T and high- T results. Inset: same data but showing β/T instead of β .

Homogeneous system: High temperature.—In the $T/T_F \gtrsim 1$ regime, we adopt the virial expansion that has been used extensively for s -wave systems [64,65]. The grand potential Ω is expanded up to the second order in the fugacity z . The second virial coefficient is obtained by the Beth-Uhlenbeck formalism [66] with the bound state contribution discarded. This is consistent with our assumption that the formation of bimolecular complexes leads to losses that are accounted for by the complex phase shift. In the weak-interaction limit, $n\Re(v_p) \ll 1$, we obtain

$$C_v = \frac{12\pi m k_B T n^2 V [\Re(v_p)]^2}{\hbar^2}. \quad (3)$$

Defining the loss-rate coefficient β through $(dn/dt) = -\beta n^2$, we find the following from Eqs. (2) and (3):

$$\beta = -\frac{72\pi k_B}{\hbar} T \Im(v_p). \quad (4)$$

It can be seen that β is proportional to T as predicted by the Bethe-Wigner threshold law and previous high-temperature results [32]. The solid lines in the main part and inset of Fig. 1 show C_v , β , and β/T , as predicted by Eqs. (3) and (4), as a function of the temperature.

Homogeneous system: Low temperature.—In the $T/T_F \ll 1$ regime, the thermodynamics of p -wave gases is expected to be governed by many-body effects. To account for interactions and Fermi statistics, we apply p -wave Fermi liquid theory [63,67]. Working, as above, at leading-order in $n\Re(v_p)$, we obtain

$$C_v = \frac{12 \times 6^{2/3} \pi^{7/3} n^{8/3} V [\Re(v_p)]^2}{5} + \frac{2^{1/3} \pi^{5/3} m^2 k_B^2 T^2 n^{4/3} V [\Re(v_p)]^2}{3^{2/3} \hbar^4}. \quad (5)$$

The two-body contact C_v contains terms that are proportional to $n^{8/3}$ and $n^{4/3}$. This is distinct from the high-temperature regime, where C_v is proportional to n^2 . Since the Fermi temperature $T_F = (6^{2/3} \pi^{4/3} \hbar^2 n^{2/3} / 2mk_B)$ is proportional to $(n^{4/3})^{1/2}$, the loss-rate coefficient becomes

$$\beta = -\frac{144\pi k_B}{5\hbar} T_F \Im(v_p) - \frac{6\pi^3 k_B T^2}{\hbar T_F} \Im(v_p), \quad (6)$$

i.e., β contains a term that is proportional to T^0 and a term that is proportional to T^2 . This behavior should be contrasted with the linear $\beta \propto T$ scaling for $T/T_F \gg 1$. In the low-temperature regime, the many-body energy scale $k_B T_F$ governs the scaling of C_v with n and, correspondingly, the scaling of β with T . Specifically, the first constant term on the right-hand sides of Eqs. (5) and (6) arises from the interacting ground state. The second term on the right-hand sides of Eqs. (5) and (6) arises from excitations out of the ground state. The dashed line in Fig. 1 shows β , Eq. (6), as a function of the temperature. It can be seen that the T^2 term has a vanishingly small contribution for $T/T_F \lesssim 0.3$. Correspondingly, β/T increases for $T/T_F \ll 1$ with decreasing T (see the inset of Fig. 1), i.e., Eq. (6) predicts an enhancement rather than a suppression.

Homogeneous system: Intermediate temperature.—We now prove that a weakly interacting p -wave Fermi gas can only have one phase transition at extremely low temperatures, thereby justifying interpolation of the low- and high-temperature expressions in the intermediate $0.4 < T/T_F < 1$ regime. Since all the Lee-Yang zeros (LYZ) [68,69] of the noninteracting single-component Fermi gas except for the LYZ at complex infinity lie on the negative real axis away from the origin [70], only the LYZ at complex infinity may move to the positive real axis as interactions are turned on perturbatively. If $\Re(v_p)$ and $\Re(R)$ have opposite signs, there exists no weakly bound two-body state below the scattering threshold, indicating that the hypothetical transition would be to a BCS phase. Since the BCS transition temperature T_c scales as $T_F \exp\{[\pi/2k_F \Re(R)] - [\pi/2k_F^2 |\Re(v_p)|]\}$ [71–73], T_c would be several orders of magnitude smaller than T_F and thus below the temperature of interest in this work. If, on the other hand, $\Re(v_p)$ and $\Re(R)$ have the same sign, the two-body bound state energy $E_b = \hbar^2 \Re(R) / m \Re(v_p)$ is positive, indicating that the hypothetical transition would be to a BEC phase. Noting that E_b scales as \hbar^2 / ml_0^2 , which is much larger than the typical system energy $\hbar^2 k^2 / m$, the gas prepared experimentally should not support such bound states, implying that the system is far from the BEC transition. Note that our arguments do not rule out the existence of other more exotic phases. Motivated by the absence of BCS- and BEC-phase transitions in the intermediate temperature regime, we conjecture that the low- and high-temperature curves provide upper and lower bounds for $\beta(T)$ for $0.4 < T/T_F < 1$. Since the low- and high-temperature

expressions differ by only 15% at $T/T_F = 0.7$, the interpolation (the dotted lines in Fig. 1) is expected to be quite accurate.

Loss in harmonically trapped system.—The most straightforward definition of the loss-rate coefficient of an inhomogeneous system is through a local quantity $\beta(\mathbf{r})$, defined by replacing the density n by the local density $n(\mathbf{r})$. Application of this generalization to the experiment requires spatially resolved loss measurements, which may not be possible due to, e.g., limited resolution caused by the finite waist of imaging lasers. To derive broadly applicable results, we instead calculate the global loss rate by applying the local-density approximation to our results for the homogeneous system. The global loss-rate coefficient β^{trap} for the trapped system is defined through $(dn^{\text{trap}}/dt) = -\beta^{\text{trap}}(n^{\text{trap}})^2$, where the average *in situ* density $n^{\text{trap}} = N/V^{\text{trap}}$ depends on the trap volume $V^{\text{trap}} = N^2 \{ \int d^3\mathbf{r} [n(\mathbf{r})]^2 \}^{-1}$. Evaluating dN/dV^{trap} , β^{trap} naturally separates into a sum of two quantities, namely $\beta_{\text{loss}}^{\text{trap}}$ and $\beta_{\text{deform}}^{\text{trap}}$, which originate from the time derivative of N and of $(V^{\text{trap}})^{-1}$, respectively. We find [44]

$$\beta_{\text{loss}}^{\text{trap}} = -\frac{V^{\text{trap}}}{N^2} \frac{dN}{dt} = \frac{\int d^3\mathbf{r} \beta(\mathbf{r}) [n(\mathbf{r})]^2}{\int d^3\mathbf{r} [n(\mathbf{r})]^2} \quad (7)$$

and

$$\begin{aligned} \beta_{\text{deform}}^{\text{trap}} &= \frac{1}{N} \frac{dV^{\text{trap}}}{dt} \\ &= \frac{2(\int d^3\mathbf{r} r n(\mathbf{r})) (\int d^3\mathbf{r} r \beta(\mathbf{r}) [n(\mathbf{r})]^3)}{(\int d^3\mathbf{r} [n(\mathbf{r})]^2)^2} \\ &\quad - \frac{2 \int d^3\mathbf{r} r \beta(\mathbf{r}) [n(\mathbf{r})]^2}{\int d^3\mathbf{r} [n(\mathbf{r})]^2}. \end{aligned} \quad (8)$$

In Eqs. (7) and (8), $\beta(\mathbf{r})$ is the local loss-rate coefficient, evaluated at each \mathbf{r} using the properties of the homogeneous system with $k_B T_F = k_B T_F(\mathbf{r}) = (\hbar^2/2m)[6\pi^2 n(\mathbf{r})]^{2/3}$. If $T \gg T_F(\mathbf{0})$, $\beta(\mathbf{r})$ follows Eq. (4) closely for all \mathbf{r} . Since Eq. (4) has no dependence on \mathbf{r} , $\beta(\mathbf{r})$ can be pulled out of the integrand, and $\beta_{\text{loss}}^{\text{trap}} = \beta$. At lower temperatures, in contrast, $\beta_{\text{loss}}^{\text{trap}}$ receives—as discussed in more detail below—contributions from the homogeneous β for a range of different densities.

The solid line in Fig. 2(a) shows β/T_F^{trap} as a function of T/T_F^{trap} , where $T_F^{\text{trap}} = (6N)^{1/3} \hbar \bar{\omega} / k_B$ is the global Fermi temperature of the trapped system and $\bar{\omega}$ is the mean angular trap frequency. The dashed and dash-dotted lines show $\beta_{\text{loss}}^{\text{trap}}$ and $\beta_{\text{deform}}^{\text{trap}}$, respectively. It can be seen that these two terms contribute approximately equally for all temperatures considered. Even though $\beta_{\text{deform}}^{\text{trap}}$ contributes to β^{trap} , we emphasize that it characterizes the change of the trap volume (or cloud size) with time and not directly the change of the number of trapped particles with time. If

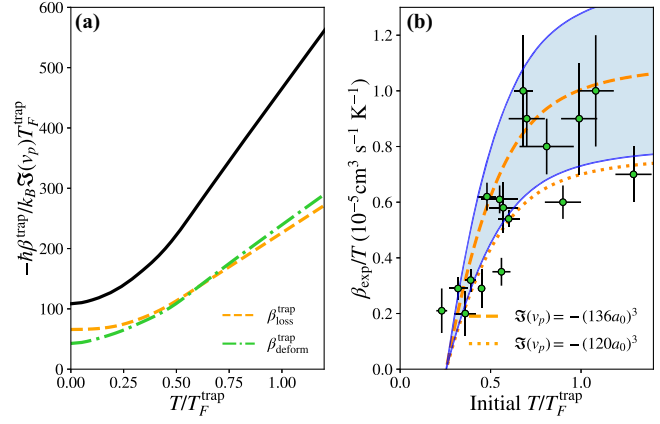


FIG. 2. (a) The black solid, orange dashed, and green dash-dotted lines show β^{trap} , $\beta_{\text{loss}}^{\text{trap}}$, and $\beta_{\text{deform}}^{\text{trap}}$ against T . (b) Theory predictions for β_{exp} (lines) are compared with measurements [24,74] (symbols) as a function of the initial temperature T . The dashed curve with the blue shaded region and the dotted curve are for $\Im(v_p) = -(136_{-14}^{+11} a_0)^3$ (extracted from [38]) and $\Im(v_p) = -(120 a_0)^3$ [30].

$[dn(\mathbf{r})/dt] \propto [n(\mathbf{r})]^\alpha$ with $\alpha > 1$, the density at the center of the cloud decreases faster than the density at the edge, causing the trap volume to increase with time.

Since both $\beta_{\text{loss}}^{\text{trap}}$ and $\beta_{\text{deform}}^{\text{trap}}$ contribute to the global loss-rate coefficient β^{trap} , experimentalists need to measure—if the gas is, as in the recent groundbreaking KRb experiment [24], prepared with an inhomogeneous density—both dN/dt and dV^{trap}/dt . To facilitate the analysis of the experimental data, Ref. [24] approximated n^{trap} by the semiclassical expression $n_{\text{exp}}^{\text{trap}}(T) = N \bar{\omega}^3 (m/\pi k_B T)^{3/2} / 8$; in addition, T in $n_{\text{exp}}^{\text{trap}}$ was approximated by T_{exp} . Both the temperature T_{exp} and particle number N were determined through ballistic expansion. With T_{exp} and N measured, dV^{trap}/dt was evaluated using $(dV^{\text{trap}}/dT_{\text{exp}})(dT_{\text{exp}}/dt)$. Finally, a loss-rate coefficient was extracted through fits. While Ref. [24]’s goal was to extract the loss-rate coefficient $\beta_{\text{loss}}^{\text{trap}}$, we refer to the experimentally extracted loss-rate coefficient as β_{exp} to remind the reader that the result relies on the use of $n_{\text{exp}}^{\text{trap}}(T_{\text{exp}})$.

The scheme described above is valid at $T \gtrsim T_F^{\text{trap}}$, where the identities $n_{\text{exp}}^{\text{trap}}(T_{\text{exp}}) = n^{\text{trap}}(T)$ and $\beta = \beta_{\text{loss}}^{\text{trap}} = \beta_{\text{exp}}$ hold. For $T \lesssim T_F^{\text{trap}}$, however, the two identities no longer hold. For example, we find that T_{exp} is twice as large as T for $T/T_F^{\text{trap}} = 0.3$; similarly, $n_{\text{exp}}^{\text{trap}}$ deviates from n^{trap} [see Fig. (S3) in the Supplemental Material [44]]. To connect our results to β_{exp} , we follow a two-step approach. First, using Eq. (4), we extract $\Im(v_p) = -(136_{-14}^{+11} a_0)^3$ from experimental high-temperature data [38], where a_0 is the Bohr radius. This is comparable to the value $-(120 a_0)^3$ obtained by multichannel quantum defect theory [30]. Second, establishing a formal connection between β^{trap}

and β_{exp} [see Eqs. (S112) and (S113) in the Supplemental Material [44]], we calculate β_{exp} over the entire temperature regime by emulating the ballistic expansion to get T_{exp} . The dashed [dotted] lines in Fig. 2(b) show our results as a function of the initial temperature T/T_F^{trap} for $\mathfrak{S}(v_p) = -(136_{-14}^{+11}a_0)^3$ [$\mathfrak{S}(v_p) = -(120a_0)^3$]. Our theory predictions agree within error bars with the experimental data.

In summary, we theoretically studied the temperature dependence of the contact and loss rate of a homogeneous Fermi gas with weak p -wave interactions parametrized by the complex p -wave scattering volume in the normal phase. In the quantum degenerate regime, the two-body loss rate is not directly proportional to the temperature, as one would expect naively by extrapolating the high-temperature results to below the Fermi temperature, but governed by two terms: one term that is directly proportional to T^2 and another term that is independent of T . Applying the local-density approximation, our parameter-free loss-rate coefficient predictions for the harmonically trapped system are found to agree with experimental measurements for a molecular KRb gas over the entire temperature regime considered. In addition, our theory framework identifies the physical origin of the leading-order behaviors within a transparent unified picture, resolving the important—yet puzzling—experimental observation that the $\beta \propto T$ scaling law does not hold below the Fermi temperature.

Our work is expected to stimulate further theoretical and experimental works at finite temperatures near the Fermi temperature. For example, our theory study lays the foundation for developing robust experimental temperature calibration schemes. We emphasize that our theoretical framework and predictions for the contact are universal, i.e., they are also applicable to single-component atomic gases, including ${}^6\text{Li}$ and ${}^{40}\text{K}$. Thus, our theory can be further verified using atomic gas experiments.

We thank Jun Ye and Junru Li for very useful discussions and information. This work is supported by the National Natural Science Foundation of China under Grant No. 12204395 and CUHK Direct Grants No. 4053583 and No. 4053535. D.B. acknowledges support by the National Science Foundation (NSF) through Grant No. PHY-2110158.

*yqyan@cuhk.edu.hk

- [1] R. Zadoyan, D. Kohen, D. A. Lidar, and V. A. Apkarian, The manipulation of massive ro-vibronic superpositions using time-frequency-resolved coherent anti-Stokes Raman scattering (TFRCARS): From quantum control to quantum computing, *Chem. Phys.* **266**, 323 (2001).
- [2] D. DeMille, Quantum Computation with Trapped Polar Molecules, *Phys. Rev. Lett.* **88**, 067901 (2002).
- [3] A. André, D. DeMille, J. M. Doyle, M. D. Lukin, S. E. Maxwell, P. Rabl, R. J. Schoelkopf, and P. Zoller, A coherent all-electrical interface between polar molecules and mesoscopic superconducting resonators, *Nat. Phys.* **2**, 636 (2006).
- [4] P. Rabl, D. DeMille, J. M. Doyle, M. D. Lukin, R. J. Schoelkopf, and P. Zoller, Hybrid Quantum Processors: Molecular Ensembles as Quantum Memory for Solid State Circuits, *Phys. Rev. Lett.* **97**, 033003 (2006).
- [5] L. D. Carr, D. DeMille, R. V. Krems, and J. Ye, Cold and ultracold molecules: Science, technology and applications, *New J. Phys.* **11**, 055049 (2009).
- [6] K. Osterloh, N. Barberán, and M. Lewenstein, Strongly Correlated States of Ultracold Rotating Dipolar Fermi Gases, *Phys. Rev. Lett.* **99**, 160403 (2007).
- [7] H. P. Büchler, E. Demler, M. Lukin, A. Micheli, N. Prokof'ev, G. Pupillo, and P. Zoller, Strongly Correlated 2D Quantum Phases with Cold Polar Molecules: Controlling the Shape of the Interaction Potential, *Phys. Rev. Lett.* **98**, 060404 (2007).
- [8] A. V. Gorshkov, S. R. Manmana, G. Chen, J. Ye, E. Demler, M. D. Lukin, and A. M. Rey, Tunable Superfluidity and Quantum Magnetism with Ultracold Polar Molecules, *Phys. Rev. Lett.* **107**, 115301 (2011).
- [9] M. A. Baranov, M. Dalmonte, G. Pupillo, and P. Zoller, Condensed matter theory of dipolar quantum gases, *Chem. Rev.* **112**, 5012 (2012).
- [10] A. Micheli, G. K. Brennen, and P. Zoller, A toolbox for lattice-spin models with polar molecules, *Nat. Phys.* **2**, 341 (2006).
- [11] J. L. Bohn, A. M. Rey, and J. Ye, Cold molecules: Progress in quantum engineering of chemistry and quantum matter, *Science* **357**, 1002 (2017).
- [12] M. T. Hummon, M. Yeo, B. K. Stuhl, A. L. Collopy, Y. Xia, and J. Ye, 2D Magneto-Optical Trapping of Diatomic Molecules, *Phys. Rev. Lett.* **110**, 143001 (2013).
- [13] J. F. Barry, D. J. McCarron, E. B. Norrgard, M. H. Steinecker, and D. DeMille, Magneto-optical trapping of a diatomic molecule, *Nature (London)* **512**, 286 (2014).
- [14] L. Anderegg, B. L. Augenbraun, E. Chae, B. Hemmerling, N. R. Hutzler, A. Ravi, A. Collopy, J. Ye, W. Ketterle, and J. M. Doyle, Radio Frequency Magneto-Optical Trapping of CaF with High Density, *Phys. Rev. Lett.* **119**, 103201 (2017).
- [15] S. Truppe, H. J. Williams, M. Hambach, L. Caldwell, N. J. Fitch, E. A. Hinds, B. E. Sauer, and M. R. Tarbutt, Molecules cooled below the Doppler limit, *Nat. Phys.* **13**, 1173 (2017).
- [16] L. Anderegg, B. L. Augenbraun, Y. Bao, S. Burchesky, L. W. Cheuk, W. Ketterle, and J. M. Doyle, Laser cooling of optically trapped molecules, *Nat. Phys.* **14**, 890 (2018).
- [17] K.-K. Ni, S. Ospelkaus, M. De Miranda, A. Pe'Er, B. Neyenhuis, J. Zirbel, S. Kotochigova, P. Julienne, D. Jin, and J. Ye, A high phase-space-density gas of polar molecules, *Science* **322**, 231 (2008).
- [18] J. W. Park, S. A. Will, and M. W. Zwierlein, Ultracold Dipolar Gas of Fermionic ${}^{23}\text{Na}{}^{40}\text{K}$ Molecules in Their Absolute Ground State, *Phys. Rev. Lett.* **114**, 205302 (2015).
- [19] F. Seeßelberg, N. Buchheim, Z.-K. Lu, T. Schneider, X.-Y. Luo, E. Tiemann, I. Bloch, and C. Gohle, Modeling the adiabatic creation of ultracold polar ${}^{23}\text{Na}{}^{40}\text{K}$ molecules, *Phys. Rev. A* **97**, 013405 (2018).

- [20] T. Takekoshi, L. Reichsöllner, A. Schindewolf, J. M. Hutson, C. R. Le Sueur, O. Dulieu, F. Ferlaino, R. Grimm, and H.-C. Nägerl, Ultracold Dense Samples of Dipolar RbCs Molecules in the Rovibrational and Hyperfine Ground State, *Phys. Rev. Lett.* **113**, 205301 (2014).
- [21] P. K. Molony, P. D. Gregory, Z. Ji, B. Lu, M. P. Köppinger, C. R. Le Sueur, C. L. Blackley, J. M. Hutson, and S. L. Cornish, Creation of Ultracold $^{87}\text{Rb}^{133}\text{Cs}$ Molecules in the Rovibrational Ground State, *Phys. Rev. Lett.* **113**, 255301 (2014).
- [22] M. Guo, B. Zhu, B. Lu, X. Ye, F. Wang, R. Vexiau, N. Bouloufa-Maafa, G. Quéméner, O. Dulieu, and D. Wang, Creation of an Ultracold Gas of Ground-State Dipolar $^{23}\text{Na}^{87}\text{Rb}$ Molecules, *Phys. Rev. Lett.* **116**, 205303 (2016).
- [23] T. M. Rvachov, H. Son, A. T. Sommer, S. Ebadi, J. J. Park, M. W. Zwierlein, W. Ketterle, and A. O. Jamison, Long-Lived Ultracold Molecules with Electric and Magnetic Dipole Moments, *Phys. Rev. Lett.* **119**, 143001 (2017).
- [24] L. De Marco, G. Valtolina, K. Matsuda, W. G. Tobias, J. P. Covey, and J. Ye, A degenerate Fermi gas of polar molecules, *Science* **363**, 853 (2019).
- [25] E. P. Wigner, On the behavior of cross sections near thresholds, *Phys. Rev.* **73**, 1002 (1948).
- [26] H. A. Bethe, Theory of disintegration of nuclei by neutrons, *Phys. Rev.* **47**, 747 (1935).
- [27] H. R. Sadeghpour, J. L. Bohn, M. J. Cavagnero, B. D. Esry, I. I. Fabrikant, J. H. Macek, and A. R. P. Rau, Collisions near threshold in atomic and molecular physics, *J. Phys. B* **33**, R93 (2000).
- [28] G. Quéméner and J. L. Bohn, Strong dependence of ultracold chemical rates on electric dipole moments, *Phys. Rev. A* **81**, 022702 (2010).
- [29] C. H. Greene, A. R. P. Rau, and U. Fano, General form of the quantum-defect theory. II, *Phys. Rev. A* **26**, 2441 (1982).
- [30] Z. Idziaszek and P. S. Julienne, Universal Rate Constants for Reactive Collisions of Ultracold Molecules, *Phys. Rev. Lett.* **104**, 113202 (2010).
- [31] P. He, T. Bilitewski, C. H. Greene, and A. M. Rey, Exploring chemical reactions in a quantum degenerate gas of polar molecules via complex formation, *Phys. Rev. A* **102**, 063322 (2020).
- [32] M. He, C. Lv, H.-Q. Lin, and Q. Zhou, Universal relations for ultracold reactive molecules, *Sci. Adv.* **6**, eabd4699 (2020).
- [33] Z. Yu, J. H. Thywissen, and S. Zhang, Universal Relations for a Fermi Gas Close to a p -Wave Interaction Resonance, *Phys. Rev. Lett.* **115**, 135304 (2015).
- [34] C. Luciuk, S. Trotzky, S. Smale, Z. Yu, S. Zhang, and J. H. Thywissen, Evidence for universal relations describing a gas with p -wave interactions, *Nat. Phys.* **12**, 599 (2016).
- [35] S. M. Yoshida and M. Ueda, Universal High-Momentum Asymptote and Thermodynamic Relations in a Spinless Fermi Gas with a Resonant p -Wave Interaction, *Phys. Rev. Lett.* **115**, 135303 (2015).
- [36] S.-L. Zhang, M. He, and Q. Zhou, Contact matrix in dilute quantum systems, *Phys. Rev. A* **95**, 062702 (2017).
- [37] M. He, S. Zhang, H. M. Chan, and Q. Zhou, Concept of a Contact Spectrum and Its Applications in Atomic Quantum Hall States, *Phys. Rev. Lett.* **116**, 045301 (2016).
- [38] S. Ospelkaus, K.-K. Ni, D. Wang, M. H. G. De Miranda, B. Neyenhuis, G. Quéméner, P. S. Julienne, J. L. Bohn, D. S. Jin, and J. Ye, Quantum-state controlled chemical reactions of ultracold potassium-rubidium molecules, *Science* **327**, 853 (2010).
- [39] S. H. Bauer, Four center metathesis reactions, *Annu. Rev. Phys. Chem.* **30**, 271 (1979).
- [40] W. B. Miller, S. A. Safron, and D. R. Herschbach, Molecular beam kinetics: Four atom collision complexes in exchange reactions of CsCl with KCl and KI, *J. Chem. Phys.* **56**, 3581 (1972).
- [41] M.-G. Hu, Y. Liu, D. D. Grimes, Y.-W. Lin, A. H. Gheorghe, R. Vexiau, N. Bouloufa-Maafa, O. Dulieu, T. Rosenband, and K.-K. Ni, Direct observation of bimolecular reactions of ultracold KRb molecules, *Science* **366**, 1111 (2019).
- [42] Y. Liu, M.-G. Hu, M. A. Nichols, D. D. Grimes, T. Karman, H. Guo, and K.-K. Ni, Photo-excitation of long-lived transient intermediates in ultracold reactions, *Nat. Phys.* **16**, 1132 (2020).
- [43] E. Braaten, H.-W. Hammer, and G. P. Lepage, Lindblad equation for the inelastic loss of ultracold atoms, *Phys. Rev. A* **95**, 012708 (2017).
- [44] See Supplemental Material at <http://link.aps.org/supplemental/10.1103/PhysRevLett.131.043401>, which includes a notation list, discussions on Lindblad equation and loss relation, second-order virial expansion for homogeneous and trapped systems, Landau Fermi liquid theory, local-density approximation, and reproduction of the experimental results with additional Refs. [43–56].
- [45] C. A. Bertulani, H. W. Hammer, and U. van Kolck, Effective field theory for halo nuclei: Shallow p -wave states, *Nucl. Phys. A* **712**, 37 (2002).
- [46] E. Braaten, P. Hagen, H.-W. Hammer, and L. Platter, Renormalization in the three-body problem with resonant p -wave interactions, *Phys. Rev. A* **86**, 012711 (2012).
- [47] J. M. Hutson, Feshbach resonances in ultracold atomic and molecular collisions: Threshold behaviour and suppression of poles in scattering lengths, *New J. Phys.* **9**, 152 (2007).
- [48] C. Ticknor, C. A. Regal, D. S. Jin, and J. L. Bohn, Multiplet structure of Feshbach resonances in nonzero partial waves, *Phys. Rev. A* **69**, 042712 (2004).
- [49] A. M. Zagoskin, *Quantum Theory of Many-Body Systems* (Springer, New York, 1998), Vol. 174.
- [50] A. L. Fetter and J. D. Walecka, *Quantum Theory of Many-Particle Systems* (Dover Publications, New York, 2003).
- [51] J. J. Sakurai, *Modern Quantum Mechanics, Revised Edition* (Addison-Wesley, New York, 1993).
- [52] L. D. Landau and E. M. Lifshitz, *Quantum Mechanics: Non-Relativistic Theory* (Elsevier, New York, 2013), Vol. 3.
- [53] T. Busch, B.-G. Englert, K. Rzazewski, and M. Wilkens, Two cold atoms in a harmonic trap, *Found. Phys.* **28**, 549 (1998).
- [54] K. Huang and C. N. Yang, Quantum-mechanical many-body problem with hard-sphere interaction, *Phys. Rev.* **105**, 767 (1957).
- [55] D. A. Butts and D. S. Rokhsar, Trapped fermi gases, *Phys. Rev. A* **55**, 4346 (1997).
- [56] C. J. Pethick and H. Smith, *Bose–Einstein Condensation in Dilute Gases* (Cambridge University Press, Cambridge, England, 2008).

- [57] K. Kanjilal and D. Blume, Nondivergent pseudopotential treatment of spin-polarized fermions under one- and three-dimensional harmonic confinement, *Phys. Rev. A* **70**, 042709 (2004).
- [58] K.-K. Ni, S. Ospelkaus, D. Wang, G. Quémener, B. Neyenhuis, M. H. G. de Miranda, J. L. Bohn, J. Ye, and D. S. Jin, Dipolar collisions of polar molecules in the quantum regime, *Nature (London)* **464**, 1324 (2010).
- [59] E. Braaten and L. Platter, Exact Relations for a Strongly Interacting Fermi Gas from the Operator Product Expansion, *Phys. Rev. Lett.* **100**, 205301 (2008).
- [60] E. Braaten and H. W. Hammer, Universal relation for the inelastic two-body loss rate, *J. Phys. B* **46**, 215203 (2013).
- [61] B. R. Levy and J. B. Keller, Low energy expansion of scattering phase shifts for long range potentials, *J. Math. Phys. (N.Y.)* **4**, 54 (1963).
- [62] P. Zhang, P. Naidon, and M. Ueda, Scattering amplitude of ultracold atoms near the p -wave magnetic Feshbach resonance, *Phys. Rev. A* **82**, 062712 (2010).
- [63] S. Ding and S. Zhang, Fermi-Liquid Description of a Single-Component Fermi Gas with p -Wave Interactions, *Phys. Rev. Lett.* **123**, 070404 (2019).
- [64] T.-L. Ho and E. J. Mueller, High Temperature Expansion Applied to Fermions near Feshbach Resonance, *Phys. Rev. Lett.* **92**, 160404 (2004).
- [65] X.-J. Liu, Virial expansion for a strongly correlated Fermi system and its application to ultracold atomic Fermi gases, *Phys. Rep.* **524**, 37 (2013).
- [66] E. Beth and G. E. Uhlenbeck, The quantum theory of the non-ideal gas. II. Behaviour at low temperatures, *Physica (Amsterdam)* **4**, 915 (1937).
- [67] G. Baym and C. Pethick, *Landau Fermi-liquid Theory: Concepts and Applications* (John Wiley & Sons, New York, 2008).
- [68] C. N. Yang and T. D. Lee, Statistical theory of equations of state and phase transitions. I. Theory of condensation, *Phys. Rev.* **87**, 404 (1952).
- [69] T. D. Lee and C. N. Yang, Statistical theory of equations of state and phase transitions. II. Lattice gas and Ising model, *Phys. Rev.* **87**, 410 (1952).
- [70] K. Huang, *Statistical Mechanics* (John Wiley & Sons, New York, 2008).
- [71] T.-L. Ho and R. B. Diener, Fermion Superfluids of Nonzero Orbital Angular Momentum near Resonance, *Phys. Rev. Lett.* **94**, 090402 (2005).
- [72] M. Iskin and C. A. R. Sá de Melo, Evolution from BCS to BEC Superfluidity in p -Wave Fermi Gases, *Phys. Rev. Lett.* **96**, 040402 (2006).
- [73] J. Yao and S. Zhang, Normal-state properties of a resonantly interacting p -wave Fermi gas, *Phys. Rev. A* **97**, 043612 (2018).
- [74] L. De Marco, G. Valtolina, K. Matsuda, W. Tobias, J. Covey, and J. Ye, Replication Data for: A Degenerate Fermi Gas of Polar Molecules, [10.7910/dvn/rlobhv](https://doi.org/10.7910/dvn/rlobhv) (2019).